DEUTSCHES ELEKTRONEN-SYNCHROTRON DESY

DESY 80/119
December 1980

QCD-PREDICTIONS FOR FOUR-JET FINAL STATES IN e^+e^--ANNIHILATION II: ANGULAR CORRELATIONS AS A TEST OF THE TRIPLE-GLUON COUPLING

by

J. G. Körner
Deutsches Elektronen-Synchrotron DESY, Hamburg

G. Schierholz and J. Willrodt
II. Institut für Theoretische Physik der Universität Hamburg

NOTKESTRASSE 85 · 2 HAMBURG 52

To be sure that your preprints are promptly included in the
HIGH ENERGY PHYSICS INDEX ,
send them to the following address (if possible by air mail) :

DESY
Bibliothek
Notkestrasse 85
2 Hamburg 52
Germany

DESY 80/119
December 1980

QCD-Predictions for Four-Jet Final States in e^+e^--Annihilation II: Angular Correlations as a Test of the Triple-Gluon Coupling

by

J.G. Körner

Deutsches Elektronen-Synchrotron DESY, Hamburg

G. Schierholz and J. Willrodt

II. Institut für Theoretische Physik der Universität Hamburg

Abstract

We investigate beam-event correlations and correlations within the event in e^+e^- annihilation into four jets. An interesting possibility to "measure" the triple-gluon coupling is found.

1. Introduction

In the last two years remarkable agreement between the order α_s predictions of quantum chromodynamic (QCD) and the e^+e^- annihilation data has been found. The observation of 3-jet events is being interpreted as evidence for the existence of gluons [1].

At order α_s^2 one expects also the occurrence of 4-jet events resulting from the perturbative processes $e^+e^- \to q\bar{q}gg$ and $e^+e^- \to q\bar{q}q\bar{q}$. The cross sections of these two processes have been given and discussed in refs. (2,3). Supported by these calculations *), first evidence for 4-jet events has recently been reported by various groups [5].

Four-jet events are quite interesting to study as QCD shows its full gauge structure only in order α_s^2. Despite the various qualitative and even semi-quantitative pieces of evidence in favour of QCD, there is so far no convincing proof of the validity of QCD, and it would be extremely important to experimentally verify the effects of the gluon self-couplings. Four-jet events are quite favourable to such an analysis because of the dominance of the $e^+e^- \to q\bar{q}gg$ cross section (which contains contributions from the triple-gluon coupling) over the $e^+e^- \to q\bar{q}q\bar{q}$ cross section [2].

As 4-jet events will be accumulating in the next few years, we shall look

*) The 4-jet amplitudes are also included in the event-generator programs [4] used at DESY.

into the nature of 4-jet events in closer detail. Led by the task of finding tests which emphasize the more fundamental aspects of QCD, we suggest to study beam-event correlations and correlations within the 4-jet events. The significance of the proposed tests will be underlined by comparing the QCD predictions to those of an abelian vector theory like QED.

The outline of the paper is as follows. In section 2 we briefly recapitulate the 4-jet cross-section calculation. Section 2 also contains the definition of the QED-like comparison theory. In section 3 we study polar correlations between the beam axis and several event-specific axes. For latter we choose the thrust and acoplanarity axis. In section 4 we study correlations within the hadron event. We study two classes of events separately according to whether the thrust hemispheres contain two and two jets or one and three jet(s). For the former class we study the azimuthal correlation between the two planes formed by the jets. We find a very interesting effect in the azimuthal correlation which we interpret as being due to the triple-gluon coupling. In the 3- and 1-jet configuration we study the thrust-distribution of the 3-jet side in its rest system. We also investigate the polar angle distribution of the rest frame thrust axis with the boost direction. Section 5 contains our conclusions.

2. Cross-Sections and Angular Correlations

As mentioned in the introduction it is convenient to compare the QCD results to a consistent alternative theory without the gluon self-couplings in order to accentuate the effects of the triple-gluon coupling contribution. This

cannot be achieved by simply switching off the triple-gluon coupling in QCD since the resulting amplitudes are no longer gauge invariant. A consistent alternative theory can be, however, formulated for colour triplet quarks and colour singlet gluons. We shall refer to this alternative Abelian theory as "QED" . The three-fold colour degeneracy of quarks is needed in order to be in agreement with the measured ratio R. The quark-gluon coupling constant of this QED-like theory will be adjusted so as to give the same 3-jet production cross-section as QCD. This yields

$$\alpha_{\text{"QED"}} = \frac{4}{3}\alpha_s \tag{2.1}$$

after a little colour algebra.

We can be brief in the exposition of the 4-jet cross-section calculation since a detailed account has been presented in ref. (2). Here we collect only some basic formulae.

The cross-section for $e^+e^- \to q\bar{q}gg$ $(q\bar{q}q\bar{q})$ is given by

$$d\sigma = \frac{e^4}{(2\pi)^8 2Q^6}\{p_+,p_-\}^{\mu\nu} H_{\mu\nu} \prod_{i=1}^{4} \frac{d^3p_i}{2p_i^0}\delta^{(4)}(p_+ + p_- + \sum_{k=1}^{4} p_k)\frac{1}{N_S} \,, \tag{2.2}$$

where (the virtual photon momentum) $q = (Q,o) = p_+ + p_-$. $H_{\mu\nu}$ is the hadron tensor of the final state and contains summation over final spin, colour and flavour states. For unpolarized beams the lepton tensor $\{p_+,p_-\}^{\mu\nu}$ is given by

$$\{p_+,p_-\}^{\mu\nu} = p_+^\mu p_-^\nu + p_-^\mu p_+^\nu - g^{\mu\nu}\frac{Q^2}{2} \,. \tag{2.3}$$

N_s is a statistical factor which is 2 (4) for $e^+e^- \longrightarrow q\bar{q}gg$ $(q\bar{q}q\bar{q})$ if all quarks are identical. Since we are working in the overall c.m. system we shall be only concerned with the spatial components of $H_{\mu\nu}$ and the lepton tensor since the time components vanish due to current conservation.

Equation (2.2) contains all beam-event correlations to be discussed in the next section. In case one is only interested in total rates eq. (2.2) simplifies to

$$d\sigma = \frac{e^4}{(2\pi)^8 2Q^6}\left(-\tfrac{2}{3}g^{\mu\nu}H_{\mu\nu}\right)\prod_{i=1}^{4}\frac{d^3p_i}{2p_i^0}\,\delta^{(4)}(p_+ + p_- - \sum_{k=1}^{4}p_k)\,\frac{1}{N_s}\,. \qquad (2.4)$$

The hadron tensor $H_{\mu\nu}$ was given in ref. (2) for $e^+e^- \longrightarrow q\bar{q}gg$. In Appendix A we shall also give $H_{\mu\nu}$ for $e^+e^- \longrightarrow q\bar{q}q\bar{q}$.

In calculating the various cross sections and angular distributions the necessary phase space integrations have been done by a Monte Carlo program.

3. Beam-Event Correlations

In this section we shall be considering beam-event correlations. The decomposition of the 4-jet cross-section into its angular parts involves 6 helicity cross sections (structure functions). One has

$$2\pi\frac{d^2\sigma}{d\chi\, d\cos\Theta} = \tfrac{3}{8}(1+\cos^2\Theta)\sigma_u + \tfrac{3}{4}\sin^2\Theta\,\sigma_L + \tfrac{3}{4}\sin^2\Theta\cos 2\chi\,\sigma_{TR} + \tfrac{3}{4}\sin^2\Theta\sin 2\chi\,\sigma_{TI} + \tfrac{3}{2\sqrt{2}}\sin 2\Theta\cos\chi\,\sigma_{IR} + \tfrac{3}{\sqrt{2}}\sin 2\Theta\sin\chi\,\sigma_{II}\,, \qquad (3.1)$$

where Θ and $\pi-\chi$ are the polar and azimuthal angles of the beam axis in the event frame as shown in fig. 1. Thus the measurement of lepton-hadron correlations allows one to determine six correlation coefficients corresponding to the 6 helicity cross-sections in (3.1). These could then be compared to theoretical predictions. Let us mention that the inclusion of transverse beam polarization effects does not enlarge the above set of 6 independent correlation coefficients. However, in this case a third angular dependence enters into the decomposition (3.1) which may help in practice to disentangle the 6 cross-sections.

A measurement of the six correlation coefficients in (3.1) would require a large 4-jet data set which is not likely to become available in the immediate future. We therefore integrate out the azimuthal dependence and remain with the single differential distribution

$$\frac{d\sigma}{d\cos\Theta} = \tfrac{3}{8}(1+\cos^2\Theta)\sigma_u + \tfrac{3}{4}\sin^2\Theta\,\sigma_L\,. \qquad (3.2)$$

Writing this as

$$\frac{d\sigma}{d\cos\Theta} \simeq 1 + \alpha\cos^2\Theta\,, \qquad (3.3)$$

one has ($\sigma = \sigma_U + \sigma_L$)

$$\alpha = \frac{\sigma_U - 2\sigma_L}{\sigma_U + 2\sigma_L} = \frac{\sigma - 3\sigma_L}{\sigma + \sigma_L} \tag{3.4}$$

Any convenient event axis can be chosen to describe the polar distribution [6]. Two choices that we will be considering are the thrust axis and the acoplanarity axis. The corresponding α's will be denoted by α_T and α_A. While (cf. (2.4))

$$\sigma = \frac{e^4}{(2\pi)^8 2Q^6} \int_{cuts} \prod_{i=1}^{4} \frac{d^3p_i}{2p_i^0} \delta^{(4)}(q - \sum_{k=1}^{4} p_k)\left(-\tfrac{2}{3} g^{\mu\nu} H_{\mu\nu}\right) , \tag{3.5}$$

a little algebra gives

$$\sigma_L = \frac{e^4}{(2\pi)^8 2Q^6} \int_{cuts} \prod_{i=1}^{4} \frac{d^3p_i}{2p_i^0} \delta^{(4)}(q - \sum_{k=1}^{4} p_k)\left(\tfrac{2}{3} e_i H_{ij} e_j\right) , \tag{3.6}$$

where $\vec{e}$ is the unit vector in the direction of the thrust and acoplanarity axis, respectively.

We introduce an acoplanarity cut $A_c = 0.05$ which defines our sample of 4-jet events entering the computation of α_T and α_A. Four-jet events with $A \geq 0.05$ can be credibly calculated within perturbation theory since one is effectively suppressing the large logarithmic contributions originating from close to mass-shell propagation of internal quarks and gluons [2].

In fig. 2 and fig. 3 we show α_T and α_A as functions of thrust. This is done separately for $q\bar{q}gg$ and $q\bar{q}q\bar{q}$ final states. Since $\sigma(e^+e^- \to q\bar{q}gg)$

dominates $\sigma(e^+e^- \to q\bar{q}q\bar{q})$ by a factor of, approximately, 10 [2], the total sample gives a value very close to $\alpha(q\bar{q}gg)$. For comparison we also have plotted the corresponding α's for 3-jet events [7]. At larger T α_T $(q\bar{q}gg)$ is very close to the 3-jet values whereas for $T \lesssim 0.65$ α_T $(q\bar{q}gg)$ becomes negative *) which, however, will be hard to test since the cross section is small in this region. The acoplanarity-axis distribution, on the other hand, looks quite different from the 3-jet case **) (where the acoplanarity axis is the normal to the event plane). In both cases $\alpha(q\bar{q}q\bar{q})$ shows quite a different behaviour.

For the weighted averages $\langle\alpha_T\rangle$ and $\langle\alpha_A\rangle$ we find

	Process	$\langle\alpha_T\rangle$	$\langle\alpha_A\rangle$
QCD	$e^+e^- \to q\bar{q}gg$	0.63	- 0.67
	$e^+e^- \to q\bar{q}q\bar{q}$	- 0.02	- 0.90
	total	0.57	- 0.69
"QED"	$e^+e^- \to q\bar{q}gg$	0.55	- 0.68
	$e^+e^- \to q\bar{q}q\bar{q}$	- 0.02	- 0.88
	total	0.30	- 0.77

(3.7)

This is to be compared to $\langle\alpha_T\rangle = 0.92$ and $\langle\alpha_A\rangle = -\frac{1}{3}$ for 3-jet

*) Note that $\frac{2}{3} \leq T \leq 1$ for three jets and $\frac{1}{\sqrt{3}} \leq T \leq 1$ for four jets.

**) The acoplanarity cut limits T to values below one .

events. For the Abelian vector theory ("QED") $\langle \alpha_T \rangle$ comes out to be significantly smaller which is mainly due to the fact that the $q\bar{q}q\bar{q}$ mode contributes $\approx$ 45 % to the total rate ($A \geq 0.05$).

4. Correlations within the events

In this section we consider correlations within the hadron events. For this purpose we integrate out all beam-event angles and consider the total cross section $\sigma = \sigma_U + \sigma_L$ which is simply given by the trace of the hadron tensor (cf. Eq. (2.4)).

We shall consider two classes of events. The first class contains two jets each in the two thrust hemispheres (fig. 4) and the second class contains one and three jets, respectively, in the two thrust hemispheres (fig. 5). Experimentally this corresponds to the observation of two broad and planar back-to-back jets in the former case and of a broad non-planar jet opposite a narrow jet in the latter case. These two classes of events will be discussed in turn.

Class I events: Two broad planar back-to-back jets

The following procedure will be used to define these events (fig. 4). First determine the overall thrust axis and then demand that the invariant mass squared in each hemisphere exceeds a given value M^2, i.e. (L left, R right),

$$\Big(\sum_{i\in L,R} E_i\Big)^2 - \Big(\sum_{i\in L,R} p_{i\parallel}\Big)^2 = \Big(\sum_{i\in L,R} E_i\Big)^2 - T^2\frac{Q^2}{4} \geq M^2. \qquad (4.1)$$

M should not be chosen too small for two reasons. First, one wants to have a clear 2-jet structure in each hemisphere which suggests $M \geq 6$ GeV. Secondly, one must be far enough away from the soft and collinear singularities at M = 0 in order for a perturbative calculation to be credible. To be on the safe side we shall use a rather large value for M, namely $M^2/Q^2 = 0.05$. Note that this cut will effectively remove the background from 2- and 3-jet events. The above cut-off leads to the cross sections

	QCD		"QED"	
$e^+e^- \rightarrow$	$q\bar{q}gg$	$q\bar{q}q\bar{q}$	$q\bar{q}gg$	$q\bar{q}q\bar{q}$
$\frac{\sigma(M)}{\sigma_0}$	0.024	0.002	0.018	0.016

(4.2)

at Q = 40 GeV and for Λ = 0.5 GeV, N_f = 5 which corresponds to $\alpha_s = 0.187$. Apart from $\ln Q^2$ variations of α_s this will be the cross section for all energies.

In the following we are going to investigate azimuthal correlations. This excludes the use of acoplanarity cuts as in section 3.

The respective 2-jet planes in opposite hemispheres allow one to define (and measure) an azimuthal angle ϕ between the normals of the two respective planes (fig. 6). The two normals can be oriented by flavour identification (e.g., $\vec{n} = \vec{p}_q \times \vec{p}_g$) or by energy ordering (e.g., $\vec{n} = \vec{p}_{\text{fastest}} \times \vec{p}_{\text{second fastest}}$) in the two respective 2-jet planes.

In order to be able to assess purely kinematical effects we plot the phase space Φ-distribution in fig. 7 using the same mass cut as above, i.e., $M^2 = 0.05\ Q^2$. The depletion of the distribution close to $\Phi = 0^\circ$ is kinematic in origin and can be understood from the following remarks. Between $M^2 = \frac{1}{8} Q^2$ and $M^2 = \frac{1}{6} Q^2$ all events have to be nonplanar. $M^2 = \frac{1}{8} Q^2$ is the largest value that can be reached by planar events, and $M^2 = \frac{1}{6} Q^2$ is the largest M^2 possible which occurs for the tetrahedron configuration. Below $M^2 = \frac{1}{8} Q^2$ one has azimuthal symmetry. However, since one is cutting out large portions of this azimuthally symmetric region and effectively enhancing the nonplanar region, this explains the behaviour of the Φ-distribution in fig. 7.

Before discussing our results let us argue what correlations can be expected and why they are interesting to be studied. In the leading log approximation ($\sim \log^4$, 2-jet limit) there will be two back-to-back (qg) and ($\bar{q}g$) pairs. One can check by a simple double-decay correlation calculation that no transverse information is communicated between the two pairs, i.e., there will be no correlation between the planes in this approximation. Correlations can come only from nonleading effects which are enhanced by our mass cuts. Let us qualitatively discuss the dominant sample of two back-to-back (qg) and ($\bar{q}g$) jets at the $\log^2$ level (corresponding to the leading log corrections to three jets).In the Feynman gauge the leading diagrams are those shown in fig. 8. In "QED" only the diagrams of fig. 8a are present. At the leading log level there are no azimuthal correlations coming from the "QED" diagrams so that the Φ-distribution should be similar to the phase-space distribution (if subleading contributions were to be neglected). The QCD diagrams (fig. 8b), on the other hand, are expected to give rise to a strong azimuthal correlation because the dominant contribution comes, moreover, from small invariant masses of the internal gluon which favours small relative angles between the gluons as well as between quark/antiquark and gluons (collinear singularity). As a result, the two jet planes will predominantly be parallel in this case.

Let us first consider non-oriented normals. This gives rise to Φ-distributions which are symmetric with respect to $\Phi \to \pi - \Phi$ (fig. 6). In figs. 9a and 9b we plot results for QCD and "QED" separately for $q\bar{q}gg$ and $q\bar{q}q\bar{q}$ final states.*) In QCD the $q\bar{q}gg$ distribution clearly dominates and shows a depletion around $\Phi = 90^\circ$ which means that the two planes tend to be aligned rather than perpendicular to one another. In "QED" the $q\bar{q}gg$ distribution is rather flat which deviates from QCD as well as from phase space. That it deviates from phase space has its origin in nonleading contributions which we will come back to. In "QED" the relative weight of the $q\bar{q}q\bar{q}$ contribution is significantly larger. In both cases the $q\bar{q}q\bar{q}$ distribution looks very similar to the phase space distribution.

In fig. 10 we show the total (non-oriented normals) 4-jet distribution for QCD and "QED" which are strikingly different for two reasons. The first reason is the absence of the triple-gluon coupling in "QED", and the second reason is the somewhat larger $q\bar{q}q\bar{q}$ contribution in "QED". If we introduce

$$A = \frac{\left(\int_0^{45^\circ} + \int_{135^\circ}^{180^\circ} - \int_{45^\circ}^{135^\circ} \right) d\Phi \frac{d\sigma}{d\Phi}}{\int_0^{180^\circ} d\Phi \frac{d\sigma}{d\Phi}} \qquad (4.3)$$

as a measure of the asymmetry of the distribution we see the difference between QCD and "QED" quite clearly. We obtain for the mass cut given above

*) In all our calculations we have assumed massless quarks. In the inner quark loop we have taken only three flavours into account since the contribution from high-mass quarks is largely suppressed.

QCD	$q\bar{q}gg$	0.11
	$q\bar{q}q\bar{q}$	- 0.08
"QED"	$q\bar{q}gg$	$\approx$ 0
	$q\bar{q}q\bar{q}$	- 0.09
phase space		- 0.09

(4.4)

In total this gives $A_{QCD} = 0.1$ and $A_{"QED"} = -0.04$. Experimentally, it should be easier to measure A than the full distribution.

We checked that for our choice of M the two gluons never get closer than 20°. This implies that we are still far enough away from the $g \to gg$ collinear singularity for a perturbative treatment to be valid.

If one would be able to distinguish between quark and gluon jets, and may be we will one day, this "gluon alignment" could be tested further. In QCD we found that $\approx$80 % of the class I events have a quark plus gluon in one hemisphere and an antiquark plus gluon in the other. For this dominant subsample one can introduce an oriented normal by defining

$$\vec{n}_L = \vec{p}_q \times \vec{p}_g \,, \quad \vec{n}_R = \vec{p}_{\bar{q}} \times \vec{p}_g \qquad (4.5)$$

(or vice versa). The ϕ-distribution now will not be symmetric with respect to $\phi \to \pi - \phi$ anymore. The result is also shown in fig. 9. It is seen that the configuration where the azimuth between the two gluons is zero, i.e., where the two gluons are "closest" to each other, is indeed favoured.

In "QED" the unsymmetrized distribution arising from the ordering of quark and gluon momenta according to (4.5) shows an enhancement for small angles of ϕ. This is due to the quark-gluon collinear singularity corresponding to the situation where a quark and a gluon from <u>different</u> thrust hemispheres get "close" to each other. In QCD this effect is also present but buried under the leading triple-gluon coupling which favours close-by gluons, i.e., $\phi \simeq 180^{\circ}$.

We like to remark that this ordering gives only an asymmetry in case that we have a quark and a gluon in each thrust hemisphere. The other events having $q\bar{q}$ and gg in the two hemispheres are symmetric with respect to $\phi \to \pi - \phi$. They contribute, however, only $\approx$20 % to the cross section.

<u>Class II events: A broad nonplanar jet opposite a narrow jet</u>

For events of this type (fig. 5), which arise from the configuration where one quark or gluon determines the thrust axis, we are not able to define an azimuthal angle as in the case of class I events. We have instead investigated these events by looking at the (boosted) thrust distribution $d\sigma/dT^*$ where T^* is the thrust of the 3-jet system in its own rest system. This is to say, we Lorentz-boost the events into the rest system of the narrow jet and define T^* to be the thrust of the remaining three-jet system. Evidence for this type of events (with the nonplanar jet showing a three-jet structure after the boost) has recently been reported [8].

In order to obtain a finite cross section we have employed a cut on T and T^*. The cut on T is necessary to stay away from T = 1 where perturbation theory is not expected to be valid. It seems also to be useful to use a T-cut

because for large T 4-jet events cannot be distinguished from 3- or 2-jet events.

In fig. 11 we have shown $\sigma_0^{-1} d\sigma/dT^*$ for different thrust cuts. The shape of the T^*-distribution does not depend on the thrust cuts, only the magnitude does. For $T^* \to 1$ $\sigma_0^{-1} d\sigma/dT^*$ is singular due to the collinear and soft singularities of the 4-jet matrix element. For the integrated cross section we obtain

T	$\frac{1}{\sigma_0}\int_{2/3}^{0.95} dT^* \frac{d\sigma}{dT^*}$
$\lesssim 0.95$	0.13
$\lesssim 0.9$	0.05
$\lesssim 0.85$	0.022

(4.6)

The background from three-jet events would be, on the parton level, a δ-function at $T^* = 1$. So this type of events should be detectable in the same way as three-jet events in the ordinary thrust distribution $d\sigma/dT$.

We have also looked at angular distributions in the angle between the T- and T^*-axis. We found a strong cut-off dependence of this distribution. For small cut-offs the T- and T^*-axis tend to be collinear whereas for larger cut-offs (where perturbation theory is more reliable) the distribution does not seem to favour a certain angle, i.e., seems to be isotropic.

5. Conclusions

In the first part of this paper we have investigated beam-event correlations of 4-jet final states. As far as testing QCD versus "QED" is concerned, the angular distribution of the thrust axis shows the largest effect. On the other hand, the angular distribution of the acoplanarity axis deviates quite substantially from that of 3-jet events. Due to the small cross sections it will, however, be hard to measure α_T and α_A unless one sits on the Z^0 resonance.

More promising seems to look for correlations within the event. We have found that the (suitably defined) azimuthal distribution $d\sigma/d\phi$ directly "measures" the triple gluon coupling. We have not taken into account hadronization which tends to smear out distributions, and also the background from 3- and 2-jet production including hadronization has been neglected (which can be removed by appropriate cuts though). We believe, however, that it will be possible to measure directly the parton distributions as in case of the thrust distribution [9] by a cluster analysis, rather than relying on Monte Carlo simulation.

We furthermore conclude that acoplanarity cuts are not well suited to single out 4-jet events because it cuts away all nearly planar events. As we have seen, 4-jet events are predominantly planar.

We have also discussed events which have three jets in one thrust hemisphere. Boosting them into their rest system seems to be a good possibility to detect this type of events on the background of 3-jet events. For comparison with QCD we have given the thrust distributions of these events in their rest system.

Appendix A

Cross section formula for $e^+e^- \to q\bar{q}q\bar{q}$ *):

We give here the explicit cross section formula for the subprocess $e^+e^- \to q\bar{q}q\bar{q}$. We use the same notation as in ref. (2):

$$\begin{aligned} s &= p_3 \cdot p_4 & x &= p_1 \cdot p_3 \\ t &= p_2 \cdot p_3 & y &= p_1 \cdot p_4 \\ u &= p_2 \cdot p_4 & z &= p_1 \cdot p_2 \end{aligned} \qquad \text{(A1)}$$

and

$$(i,j)^{\mu\nu} = p_i^{\mu} p_j^{\nu} + p_i^{\nu} p_j^{\mu} - g^{\mu\nu} p_i \cdot p_j \quad , \; i,j = 1,\dots,4. \qquad \text{(A2)}$$

We then can write

$$H_{\mu\nu} = (4\pi\alpha_s)^2 \sum_{m \geq n = 1}^{8} A(m,n)_{\mu\nu} F(m,n) \quad , \qquad \text{(A3)}$$

where F(m,n) is the flavour matrix which has the elements (the ordering of i and j refers to the ordering of diagrams in fig. 1b , ref. (2)):

*) The matrix element has been calculated in ref.(2)but was not explicitly given there. We report the formula here for completeness.

$$\begin{aligned} F(m,n) &= N_f \sum_{k=1}^{N_f} Q_k^2 \quad \text{for } (m,n) = (1,1);(3,3);(5,5);(7,7) \\ &= \Big(\sum_{k=1}^{N_f} Q_k \Big)^2 \quad \text{for } (m,n) = (5,3);(7,1) \\ &= \sum_{k=1}^{N_f} Q_k^2 \quad \text{for } (m,n) = (3,1);(5,1);(7,3);(7,5) \end{aligned} \qquad \text{(A4)}$$

and similarly for the matrix elements where $1 \to 2$, $3 \to 4$, $5 \to 6$, $7 \to 8$.

For A(m,n) we get (dropping the tensor indices except in $g_{\mu\nu}$)

$$\begin{aligned} A(1,1) = 4\big[&(1,4)(-t^2+tx+xz) + (2,4)(tx+tz-x^2) \\ &+ (3,4)(2tx+tz+xz)\big] / z^2(t+x+z)^2 \end{aligned}$$

$$\begin{aligned} A(2,1) = 4\big[&g_{\mu\nu}(-2ty z - 2ux z) + (1,1)2tu + (2,2)2xy \\ &- (3,3)(uz+yz) - (4,4)(tz+xz) + (1,2)(2sz-2ty-2ux) \\ &+ (1,3)(sz+tu-ux-uz) + (1,4)(sz+tu-ty-tz) \\ &+ (2,3)(sz-ty+xy-yz) + (2,4)(sz-ux+xy-xz) \\ &+ (3,4)(2sz-2ty-2ux)\big] / z^2(t+x+z)(u+y+z) \end{aligned}$$

$$\begin{aligned} A(2,2) = 4\big[&(1,3)(uy+yz-u^2) + (2,3)(uy+uz-y^2) \\ &+ (3,4)(2uy+uz+yz)\big] / z^2(u+y+z)^2 \end{aligned}$$

$$A(7,1) = 4\big[\, g_{\mu\nu}(2txy + 2ux^2) + (1,1)(ux - st) + (2,2)xy + (3,3)(ux - yz)$$
$$+ (4,4)tx + (1,2)(-sx + sz - ux - xy) + (1,3)(sz + ty + ux)$$
$$+ (1,4)(-st - xz) + (2,3)(-sx - yz) + (2,4)(sz + ty - ux + 2x^2)$$
$$+ (3,4)(sz - tx - ux - xz)\,\big] / sz(s+x+y)(t+x+z)$$

$$A(7,2) = 4\big[\, g_{\mu\nu}(-2ty^2 - 2uxy) + (1,1)(su - ty) + (2,2)(-xy) + (3,3)(-uy)$$
$$+ (4,4)(xz - ty) + (1,2)(sy - sz + ty + xy) + (1,3)(su + yz)$$
$$+ (1,4)(-sz - ty - ux) + (2,3)(-sz + ty - ux - 2y^2) + (2,4)(sy + xz)$$
$$+ (3,4)(-sz + ty + uy + yz)\,\big] / sz(s+x+y)(u+y+z)$$

$$A(8,2) = 4\big[\, g_{\mu\nu}(2tuy + 2u^2x) + (1,1)tu + (2,2)(ux - sy) + (3,3)uy$$
$$+ (4,4)(ux - tz) + (1,2)(sz - su - tu - ux) + (1,3)(sz + ty + 2u^2 - ux)$$
$$+ (1,4)(-su - tz) + (2,3)(-sy - uz) + (2,4)(sz + ty + ux)$$
$$+ (3,4)(sz - ux - uy - uz)\,\big] / sz(s+t+u)(u+y+z)$$

$$A(3,1) = 4\big[\, x\,(-(1,1)u - (3,3)u + (1,2)(s+y) - (1,3)2u + (1,4)(t+z)$$
$$+ (2,3)(s+y) - (2,4)2x + (3,4)(t+z) - 2g_{\mu\nu}ux)\,\big] /$$
$$3yz(t+x+z)(s+x+y)$$

$$A(4,1) = 4\big[\, -(1,1)tu - (2,2)xy + (3,3)uz + (4,4)xz$$
$$+ (1,2)(-sz + ty + ux) + (1,3)(-tu + uz) + (1,4)(-sz + ty)$$
$$+ (2,3)(-sz + ty) + (2,4)(-xy + xz) + (3,4)(-sz + ty + ux)$$
$$+ g_{\mu\nu}\,2uxz\,\big] / 3yz(t+x+z)(u+y+z)$$

$$A(4,2) = 8\big[\, u\,((1,3)u - (2,3)(y+z) - (3,4)(y+z))\,\big] / 3yz(u+y+z)^2$$

$$A(5,1) = 8\big[\, x\,(-(1,4)(t+z) + (2,4)x - (3,4)(t+z))\,\big] / 3tz(t+x+z)^2$$

$$A(5,2) = 4\big[\, -(1,1)tu - (2,2)xy + (3,3)uz + (4,4)xz$$
$$+ (1,2)(-sz + ty + ux) + (1,3)(-tu + uz) + (1,4)(-sz + ty)$$
$$+ (2,3)(-sz + ty) + (2,4)(-xy + xz) + (3,4)(-sz + ty + ux)$$
$$+ g_{\mu\nu}\,2uxz\,\big] / 3tz(t+x+z)(u+y+z)$$

$$A(6,2) = 4\big[\, u\,(-(2,2)x - (4,4)x + (1,2)(s+t) - (1,3)2u + (1,4)(s+t)$$
$$+ (2,3)(y+z) - (2,4)2x + (3,4)(y+z) - 2g_{\mu\nu}ux)\,\big] /$$
$$3tz(u+y+z)(s+t+u)$$

(A5)

These formulae already include the colour factors. The remaining matrix elements are obtained by the following permutation of momenta:

If we interchange p_1 and p_3:

$$[A(1,1);\ A(2,1);\ A(2,2);\ A(4,1);\ A(4,2);\ A(5,2);\ A(7,1);\ A(3,1);\ A(7,2);\ A(8,2)]$$

$$\rightarrow [A(5,5);\ A(6,5);\ A(6,6);\ A(8,5);\ A(8,6);\ A(6,1);\ A(5,3);\ A(7,5);\ A(6,3);\ A(6,4)] \tag{A6}$$

Interchanging p_2 and p_4:

$$[A(1,1);\ A(2,1);\ A(2,2);\ A(4,1);\ A(5,1);\ A(5,2);\ A(6,2);\ A(7,2)]$$

$$\rightarrow [A(3,3);\ A(4,3);\ A(4,4);\ A(3,2);\ A(7,3);\ A(7,4);\ A(8,4);\ A(5,4)] \tag{A7}$$

If we interchange $p_1 \leftrightarrow p_3$ and $p_2 \leftrightarrow p_4$ we find:

$$[A(1,1);\ A(2,1);\ A(2,2);\ A(4,1);\ A(5,2);\ A(7,2)]$$

$$\rightarrow [A(7,7);\ A(8,7);\ A(8,8);\ A(7,6);\ A(8,3);\ A(8,1)] \tag{A8}$$

The calculation of the matrix element was done in the Feynman gauge using the algebraic computer program REDUCE.

References

1. TASSO Collaboration, R. Brandelik et al., Phys. Lett. 86B (1979) 243;
   MARK-J Collaboration, D.P. Barber et al., Phys. Rev. Lett. 43 (1979) 830;
   PLUTO Collaboration, Ch. Berger et al., Phys. Lett. 86B (1979) 418;
   JADE Collaboration, W. Bartel et al., Phys. Lett. 91B (1980) 142

2. A. Ali, J.G. Körner, G. Kramer, Z. Kunszt, E. Pietarinen, G. Schierholz and J. Willrodt, Phys. Lett. 82B (1979) 285 and Nucl. Phys. B167 (1980) 454

3. K.J.F. Gaemers and J.A.M. Vermaseren, CERN preprint TH-2816 (1980)

4. A. Ali, E. Pietarinen and J. Willrodt, DESY internal report T-80/01 (1980);
   A. Ali, G. Kramer, E. Pietarinen and J. Willrodt, Phys. Lett. 93B (1980) 155

5. MARK-J Collaboration, private communication;
   TASSO Collaboration, private communication;
   PLUTO Collaboration, Ch. Berger et al., DESY preprint 80/93 (1980)

6. N.M. Avram and D.H. Schiller, Nucl. Phys. B70, 272 (1974)

7. G. Kramer, G. Schierholz and J. Willrodt, Phys. Lett. 78B (1978) 249, Erratum ibid. 80B (1979) 433

8. S.L. Wu, Rapporteur Talk, Proceedings of the Arctic School of Physics, July 27 - August 5, 1980, Äkäslompolo-Lapland, Finland and DESY preprint

9. PLUTO Collaboration, ref. (5)

Figure Captions

1. Definition of polar angle Θ and azimuthal angle χ of the beam axis in the event frame. The event z-axis points into the thrust direction. The x-axis can be chosen to point into the direction of the second most energetic jet.

2. α_T as a function of T for $e^+e^- \rightarrow q\bar{q}gg$ (full line), $q\bar{q}q\bar{q}$ (dashed line) and $q\bar{q}g$ (dashed dotted line). The 3-jet curve ($q\bar{q}g$) is kinematically limited to $T \geq 2/3$.

3. α_A as a function of T for $e^+e^- \rightarrow q\bar{q}gg$ (full line), $q\bar{q}q\bar{q}$ (dashed line) and $q\bar{q}g$ (dashed dotted line).

4. Example for class I-events: Two jets in each thrust hemisphere.

5. Example of class II-events: One and three jet(s) in the two thrust hemispheres.

6. Definition of the azimuthal angle Φ : Angle between the two planes containing the two jets in the thrust hemispheres. In case of oriented normals see text.

7. Shape of the distribution $d\sigma/d\Phi$ for phase-space like events using only the invariant mass cuts. $\frac{M^2}{Q^2} \geq 0.05$ in each hemisphere. Arbitrary scale.

8. QCD diagrams for the leading contribution to 4-jet production from two back-to-back pairs. (a) Diagrams present in QCD and "QED", (b) Diagrams only present in QCD.

9. Azimuthal distribution $\sigma_0^{-1} d\sigma/d\phi$ for 4-jet production. (a) QCD. Full curve gives the distribution for $q\bar{q}gg$, the dashed-dotted curve for $q\bar{q}q\bar{q}$. The dashed curve shows the distribution for $q\bar{q}gg$ if quarks and gluons are identified and the normal of the plane is oriented as described in the text. (b) "QED" (same notation). The curves are normalized to give the correct cross sections.

10. Comparison of the total 4-jet distribution $\sigma_0^{-1} d\sigma/d\phi$ for QCD (full line) and "QED" (dashed line). Normalization as in fig.9.

11. $\sigma_0^{-1} d\sigma/dT^*$ for class-II events for different T cuts.

    I: $T \leq 0.95$

    II: $T \leq 0.9$

    III: $T \leq 0.85$

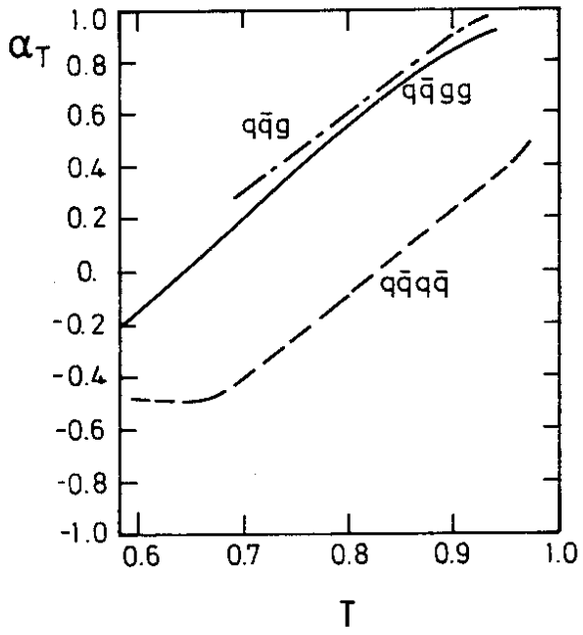

Fig. 2

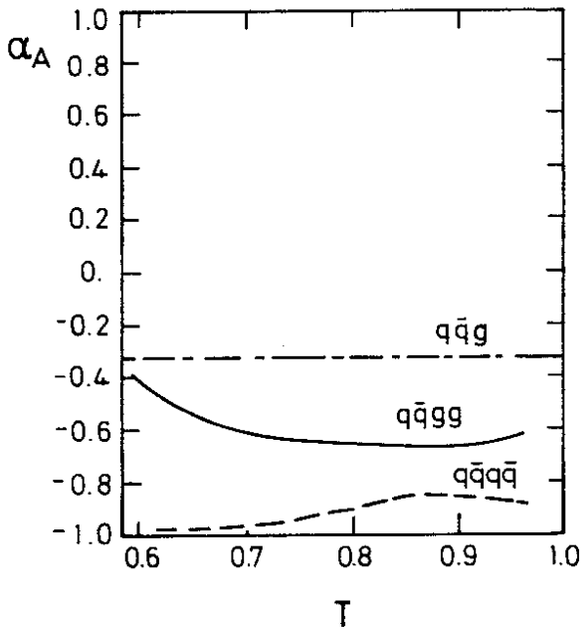

Fig. 3

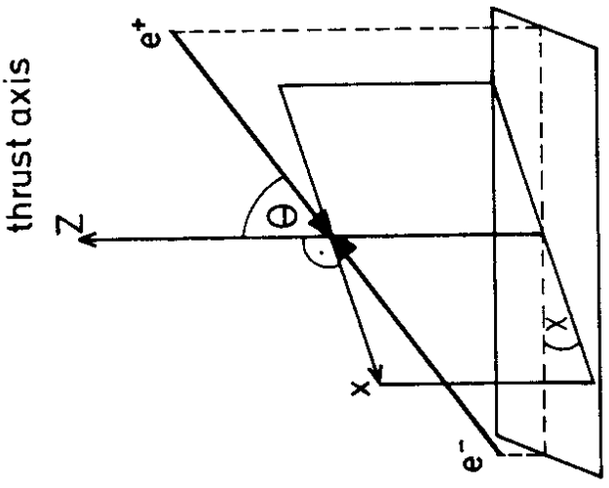

Fig. 1

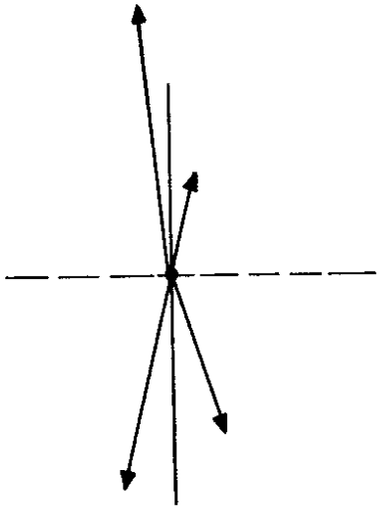

Fig. 4

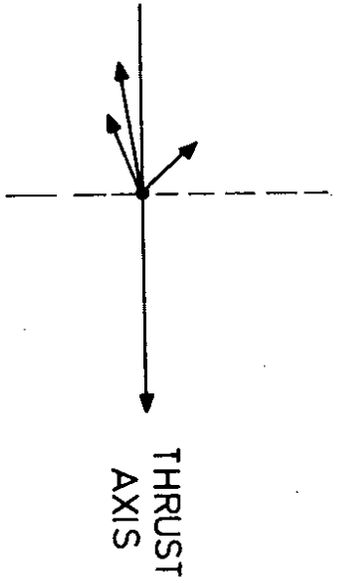

Fig. 5

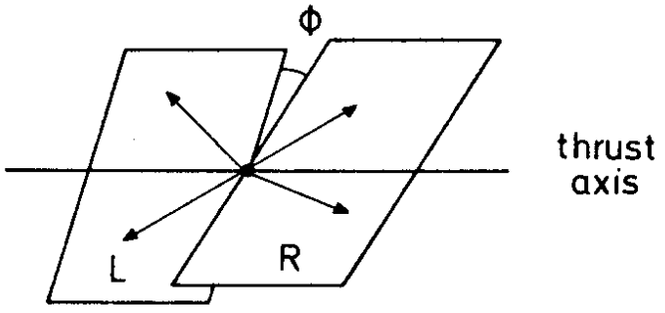

Fig. 6

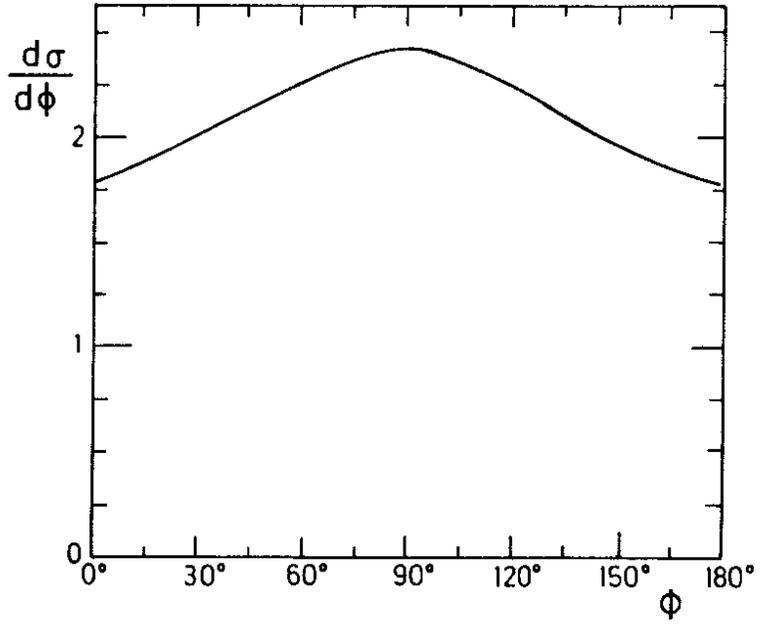

Fig. 7

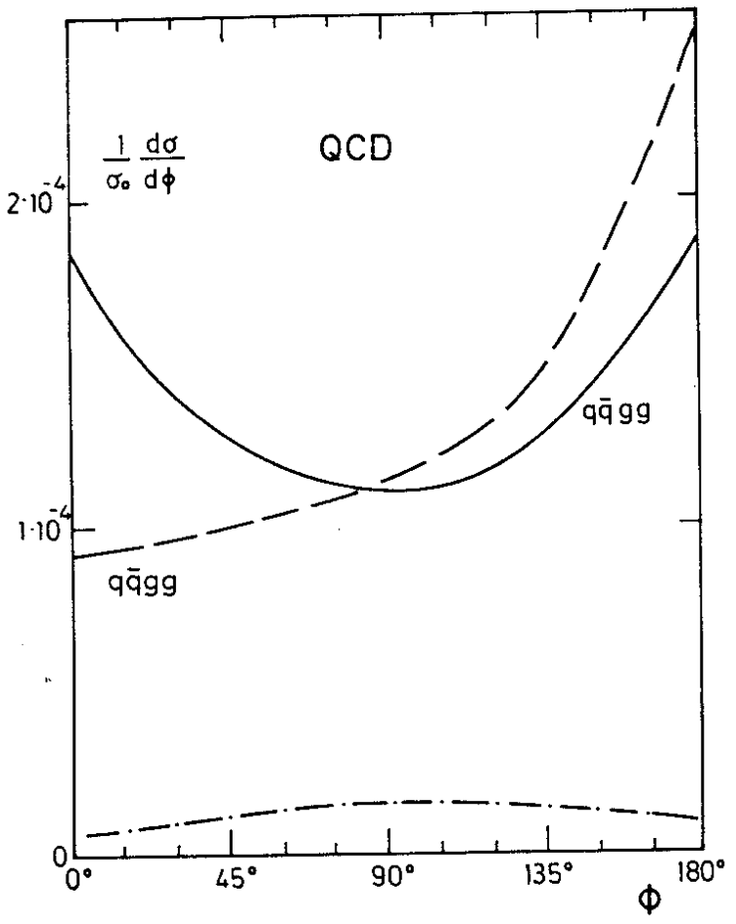

Fig. 9a

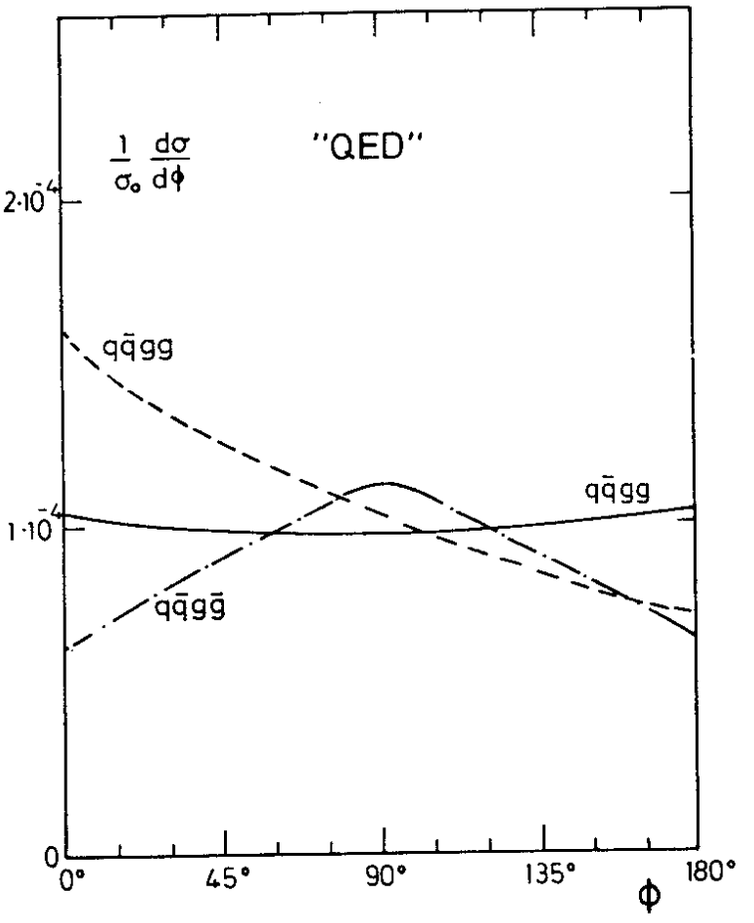

Fig.9b

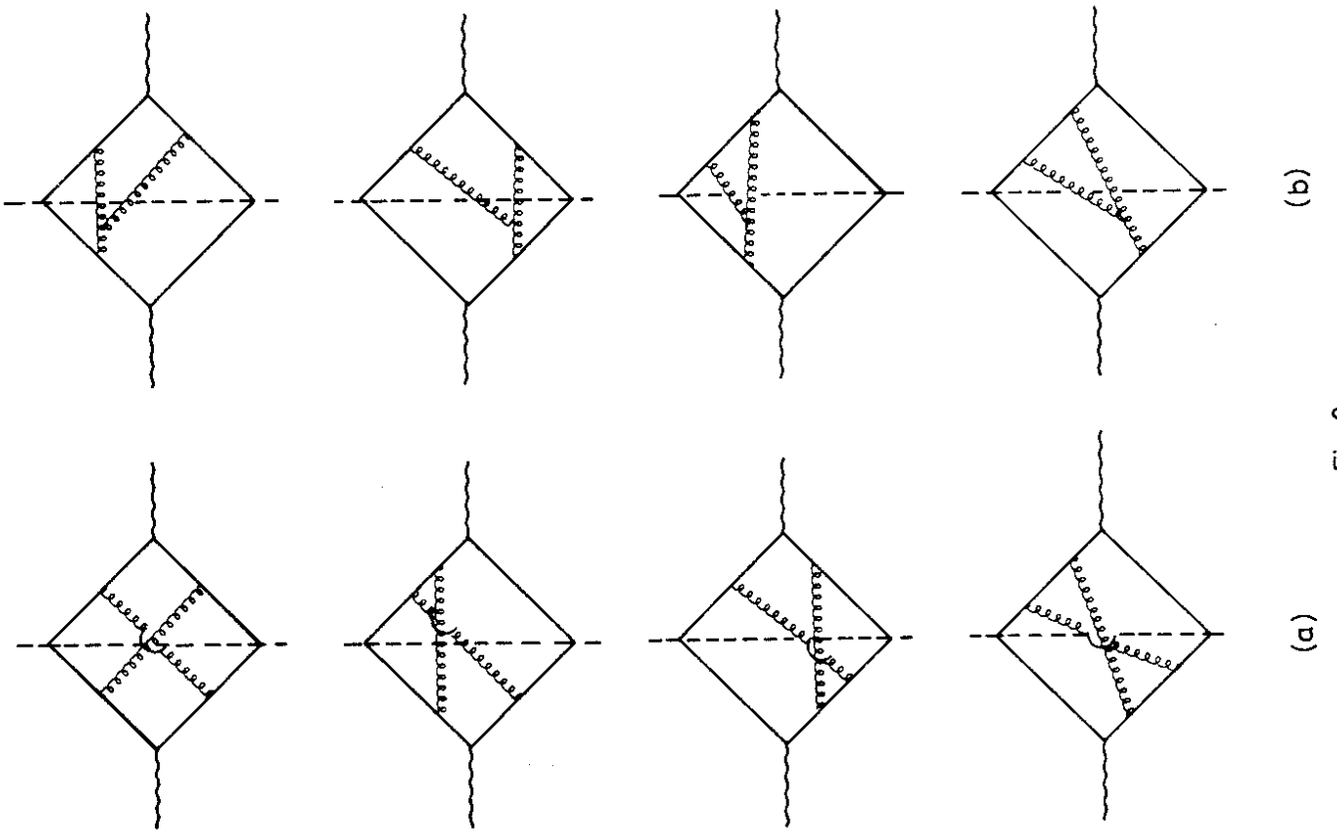

Fig.8

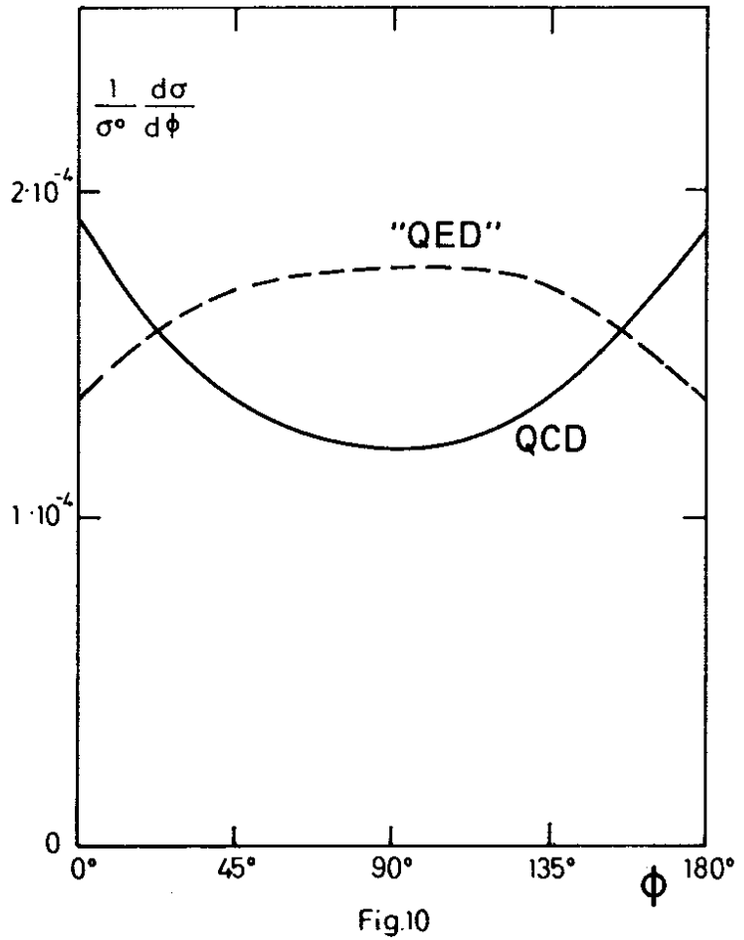
1/σ° dσ/dφ
2·10⁻⁴
1·10⁻⁴
0
"QED"
QCD
0°
45°
90°
135°
180°
φ

Fig.10

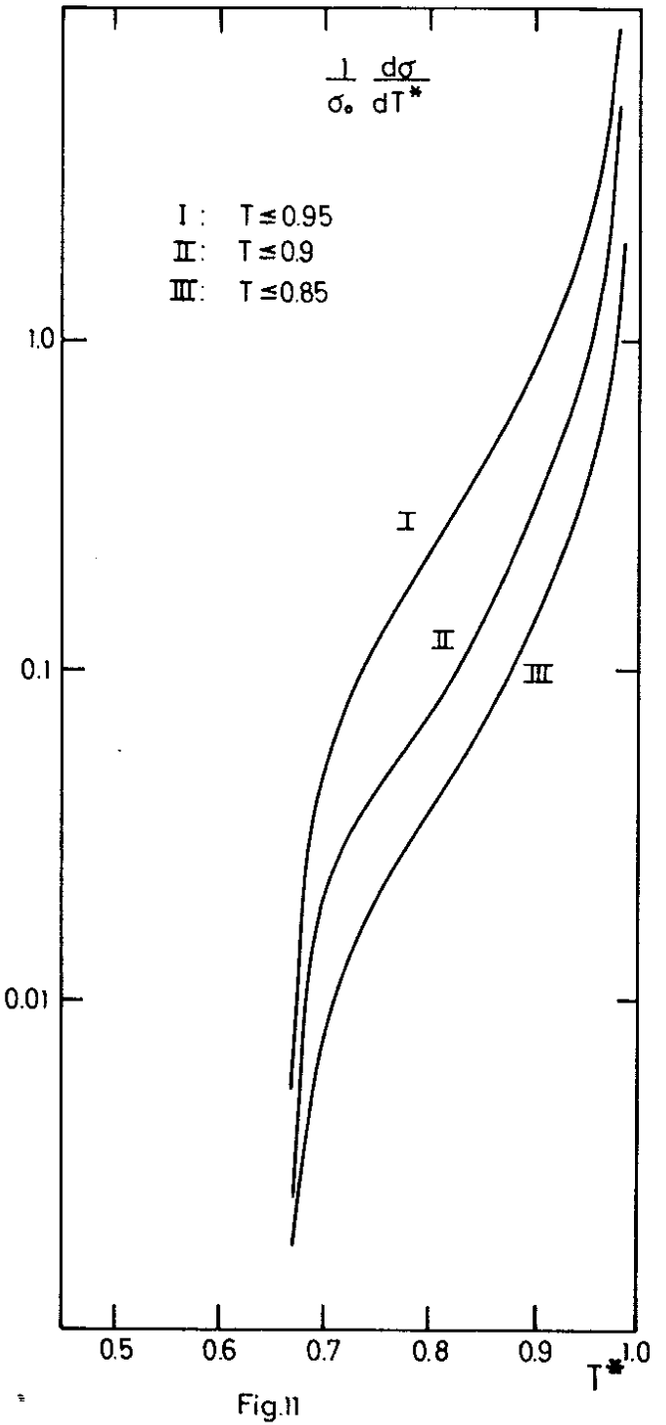
1/σ₀ dσ/dT*
I : T≤0.95
II: T≤0.9
III: T≤0.85
1.0
0.1
0.01
I
II
III
0.5
0.6
0.7
0.8
0.9
1.0
T*

Fig.11